



Lu, W. Y., Bird, T., Boulter, L., Cole, A., Hay, T., Ridgway, R. A., Kendall, T., Jamieson, T., Hay, D., Iredale, J., Clarke, A. R., & Sansom, O. J. (2015). Hepatic progenitor cells of biliary origin with liver repopulation capacity. *Nature Cell Biology*, 17(8), 971-983.
<https://doi.org/10.1038/ncb3203>

Peer reviewed version

Link to published version (if available):
[10.1038/ncb3203](https://doi.org/10.1038/ncb3203)

[Link to publication record in Explore Bristol Research](#)
PDF-document

This is the author accepted manuscript (AAM). The final published version (version of record) is available online via Springer Nature at <https://www.nature.com/articles/ncb3203> . Please refer to any applicable terms of use of the publisher.

University of Bristol - Explore Bristol Research

General rights

This document is made available in accordance with publisher policies. Please cite only the published version using the reference above. Full terms of use are available:
<http://www.bristol.ac.uk/red/research-policy/pure/user-guides/ebr-terms/>

Supplementary figure 1. Lineage tracing experiments to investigate the differentiation ability of HPCs

(a) Schematic representation showing experimental design of lineage tracing experiments using the *Krt19^{CreERT}LSL^{TdTomato}* mice. (b) Immunohistochemistry analysis for tdTomato and p21 on injured and uninjured tamoxifen induced *Krt19^{CreERT}LSL^{TdTomato}* mice. (c) Immunohistochemistry for CYP2D (green), TdTomato (red), and DAPI (blue) on liver of tamoxifen induced *Krt19^{CreERT}LSL^{TdTomato}* mice after CDE – recovery. The results shown are representative of 2 experiments with 5-8 mice each group. Scale bars = 50µm.

Supplementary figure 2. Administration of BNF induce hepatocyte damage

(a) Morphology by H&E and (b) expression of CYP2D6 by isolated purified hepatocytes following liver perfusion and digestion. Arrows denote examples of multinucleated hepatocytes. (c) Expression of nuclear p53 following extraction and purification of hepatocytes from AhCre⁺ *Mdm2*^{flox/flox} mice (n = 3) 2 days following induction with 80mg/kg βNF compared to AhCre⁻ *Mdm2*^{flox/flox} controls; arrow highlights low nuclear p53 expression. (d) Modified representation of *Mdm2*^{flox} construct outlining primer targets for qPCR assessment of recombination efficiency. (e) Serum alkaline phosphatase (f) and ALT following induction in with 80mg/kg in AhCre⁺ *Mdm2*^{flox/flox} animals (mean ± s.e.m, Kruskal Wallis Test, n = 3 mice each group, except day 8 where n=1 mouse due to cohort morbidity). (g) Expression of apoptosis associated p53-dependent gene *Bax* in whole liver over time following induction with 80mg/kg βNF in AhCre⁺ *Mdm2*^{flox/flox} mice (mean ± s.e.m, One-way ANOVA.; n=3 mice each control time point and n = 3,3,6,5 for experimental time points). (h) Immunohistochemistry for lactate dehydrogenase of healthy mice, βNF induced AhCre⁻ *Mdm2*^{flox/flox} controls and βNF induced AhCre⁺ *Mdm2*^{flox/flox} mice. Representative images shown are representative of 2 experiments with 12 mice in total. Scale bars = 50 μm

Supplementary figure 3. Activation of ductular reaction following hepatocyte damage

Detection of (a) EpCAM (b) DLK1 (c) A6 (inset, AhCre⁻ control) expressing cells following $\Delta Mdm2$ in hepatocytes. (d) Immunohistochemistry for CD24 (red), EpCAM (green), DAPI (blue) on CDE treated and β NF induced *AhCre⁺Mdm2^{flox/flox}* mice. Representative images are shown are representative of 3 experiments with 5-8 mice each group (e) *Ck19* expression in the whole liver of the induced *Mdm2^{flox/flox}* mice versus uninduced control over time (mean \pm s.e.m, One-way ANOVA with Bonferroni correction. $P=0.0058$ day 8; $n=3$ mice each control time point and $n = 3,3,6,5$ for experimental time points, repeated twice). (f) *Ascl2* expression of *Mdm2^{flox/flox}* mice over time following induction (mean \pm s.e.m, One-way ANOVA with Bonferroni correction. $P=0.05$; $n=3$ mice, repeated twice). (g) Quantitative comparison of the panCK positive cells between the uninduced control, *Mdm2^{flox/-}* *Mdm2^{flox/flox}*, and the choline deficient ethionine supplemented diet (CDE) model (mean \pm s.e.m, One-way ANOVA with Bonferroni correction. $n = 4,6,5,5$ mice each group respectively). (h) BrdU and panCK co-expressing cells can be observed 2 days after $\Delta Mdm2$. Representative images are shown are representative of 3 mice each group. Scale bars = 50 μ m.

Supplementary figure 4. Expandability of EpCAM+ CD24+ CD133+ population *in vitro*

(a) Morphology of cdHPCs after passaging with trypsin (left) or diluted trypsin (right). Insets show high magnification pictures. (b) Percentage of total EpCAM+CD24+CD133+ cells after *in vitro* expansion. (mean \pm s.e.m, n = 6 biological replicates, Mann-Whitney test) (c) mRNA expression in relative to housekeeping gene (*Ppia*) of expanded cdHPCs (mean \pm s.e.m, n= 3 biological replicates). (d) Heat map representation comparing mRNA expression in relative to housekeeping gene *Ppia* of cdHPC clones and primary hepatocytes. (e) Relative mRNA expression for HPC related genes *Lgr5*, *EpCAM*, *Albumin*, *Ck19*, *Spp1*, *Sox9* on early and late passages cdHPCs (mean \pm s.e.m, Kruskal Wallis test. $P > 0.05$, except *Lgr5* $P = 0.0286$; n=4 biological replicates). (f) Immunocytochemistry for HPC markers Sox9, CK19, OPN, and HNF1 β on early and late passages cdHPC. (g) Cell area, roundness, and width to length ratio of early and late passages cdHPCs (mean \pm s.e.m, Kruskal Wallis test $P = 0.0107$; n=4 biological replicates). (h) Calculation for the average number of cell division after 10 passages; n=3 biological replicates. Representative images represent data obtained from 3 individual experiments. Scale Bar = 100 μ m

Supplementary figure 5. Ability to differentiate towards both hepatic and biliary lineage *in vitro*

(a) FACS analysis of LGR5, CD31 and CD45 expression on *in vitro* expanded cdHPCs. Isotype control (blue line) (b) Immunocytochemistry for desmin and GFAP in *in vitro* expanded HPCs. (isolated stellate cells as positive control). (c) *In vitro* differentiation of expanded HPCs into cholangiocytes stained with activated bile duct marker MIC1C3 (green) and Hnf1 β (red), DAPI (blue). (d) *In vitro* differentiation of expanded HPCs into hepatocytes dotted line demarcates a hepatocyte like colony, upper panel. Increase Glycogen storage detected by Periodic acid-Schiff staining on differentiated cdHPCs. (e) *Alb* mRNA expression and secreted protein following hepatocyte differentiation (mean \pm s.e.m, P = 0.007 Mann-Whitney test; n=5 biological replicates). Lower histograms demonstrate expression of cholangiocyte related genes, and hepatocyte transcription factor *Hnf1 α* . Representative images are shown as representative of 3 individual experiments. Scale Bars = 50 μ m

Supplementary figure 6. Secondary clone sorting assay for the *in vitro* expanded HPCs.

(a) EpCAM and CD24 expression of *in vitro* expanded HPCs. (b) EpCAM and CD24 expression analysis of secondary clones 7 days after replating. (c) Percentage of EpCAM⁺ CD24^{Hi} population in secondary clone cultures (mean \pm s.e.m, Kruskal Wallis test; $P = 0.0076$). Data are represented as mean \pm s.e.m., n=5 biological replicates. Representative images represents 3 individual experiments.

Supplementary figure 7. Liver repopulating capacity of the *in vitro* expanded HPCs.

(a) Stitched image of GFP expressing cells in CAG-GFP HPCs transplanted animals. (b) Detection of GFP, ductular marker (panCK) and hepatocyte marker (HNF4 α) in transplanted animals and non-transplanted controls (white arrow, GFP- panCK+; red arrow, GFP+ panCK+; green arrow, GFP+ HNF4 α -; yellow arrow, GFP+ HNF4 α +). (c) Detection of GFP and proliferation marker (Ki67) or senescence marker (p21) in transplanted animals and non-transplanted controls (insets, higher magnification) three months after HPC transplantation (upper panel). (White arrows show GFP+ Ki67+ hepatocytes; Yellow arrow shows p21- GFP+ hepatocytes). Data shown here are representative of 3 experiments with 8-10 mice each group. Scale Bars = 50 μ m, except stitched image (a) where scale bar = 200 μ m.

Supplementary table 1: Recombination efficiency of the ΔMdm system and summary of experimental design

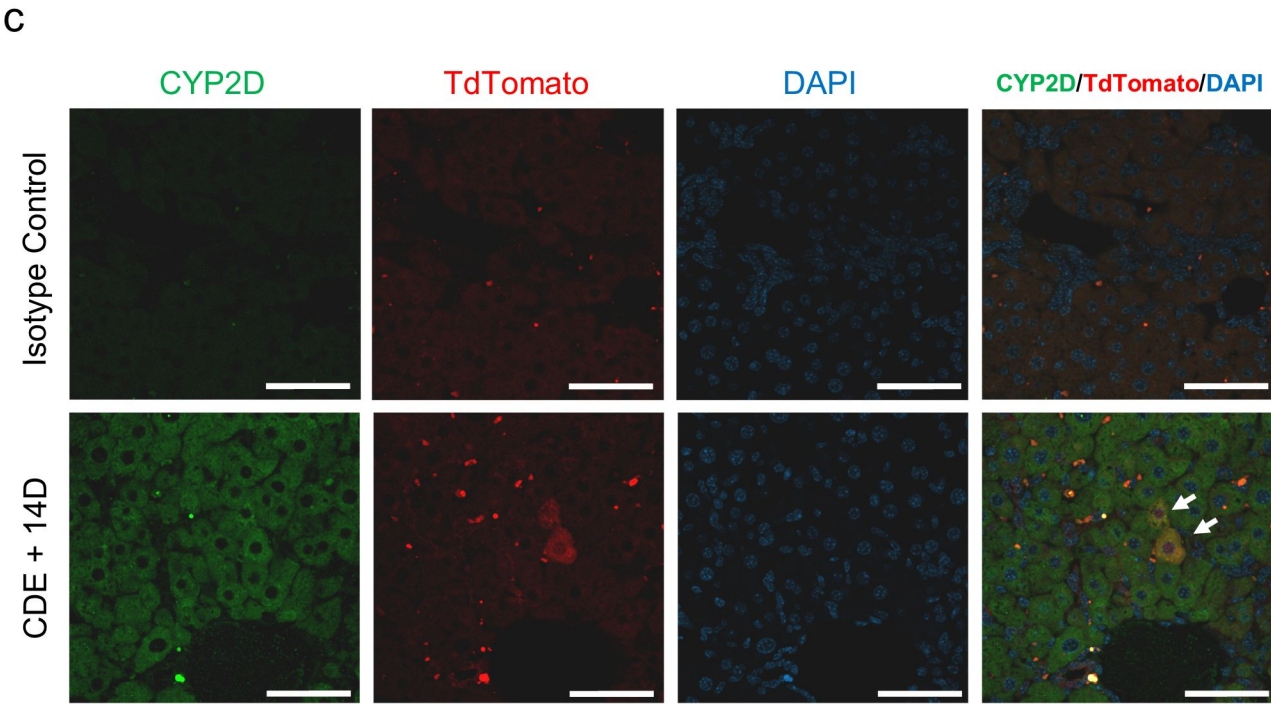
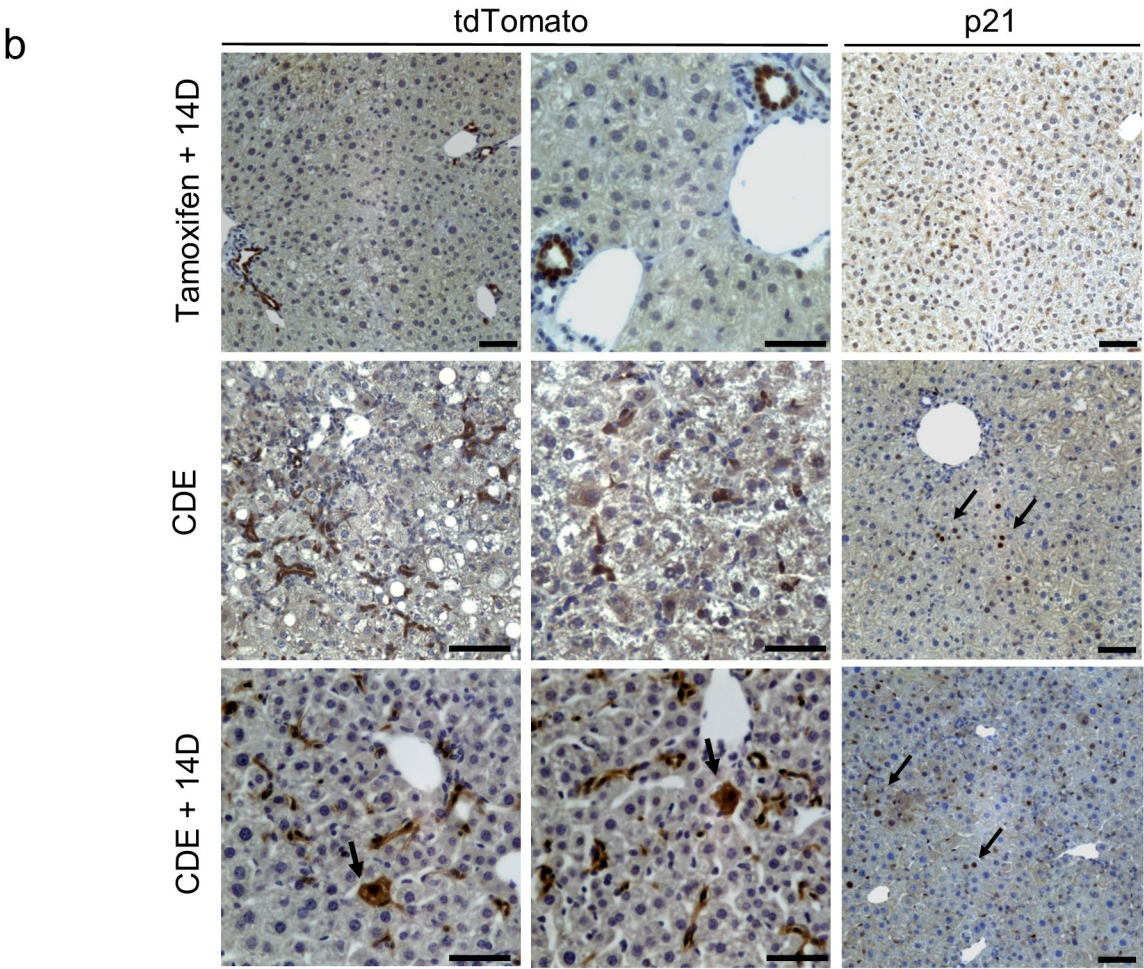
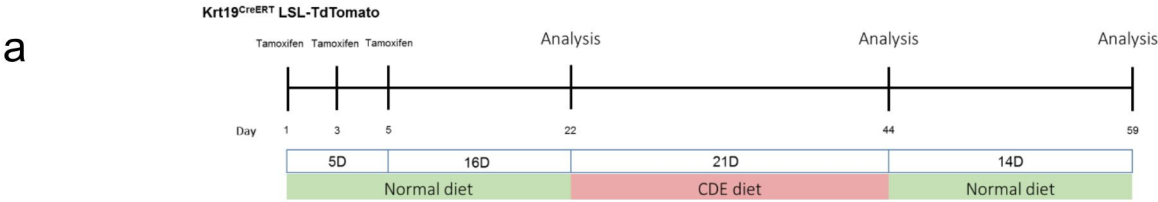
Efficiency of recombination as assessed by over-expression of nuclear p53 in hepatocytes; n≥3 each group († by qPCR of genomic DNA from purified *ex vivo* hepatocytes; see also **Supplementary Fig 1**).

No up-regulation of hepatocellular p53 was seen in uninduced AhCre⁺ *Mdm2*^{flox/flox} or AhCre⁻ *Mdm2*^{flox/+} control mice given 80mg/Kg βNF. Mice induced with 240mg/kg βNF were given 3 separate injections of 80mg/Kg βNF over 24hrs. Schematic representation of experimental design for the AhCre Δ *Mdm2* mice.

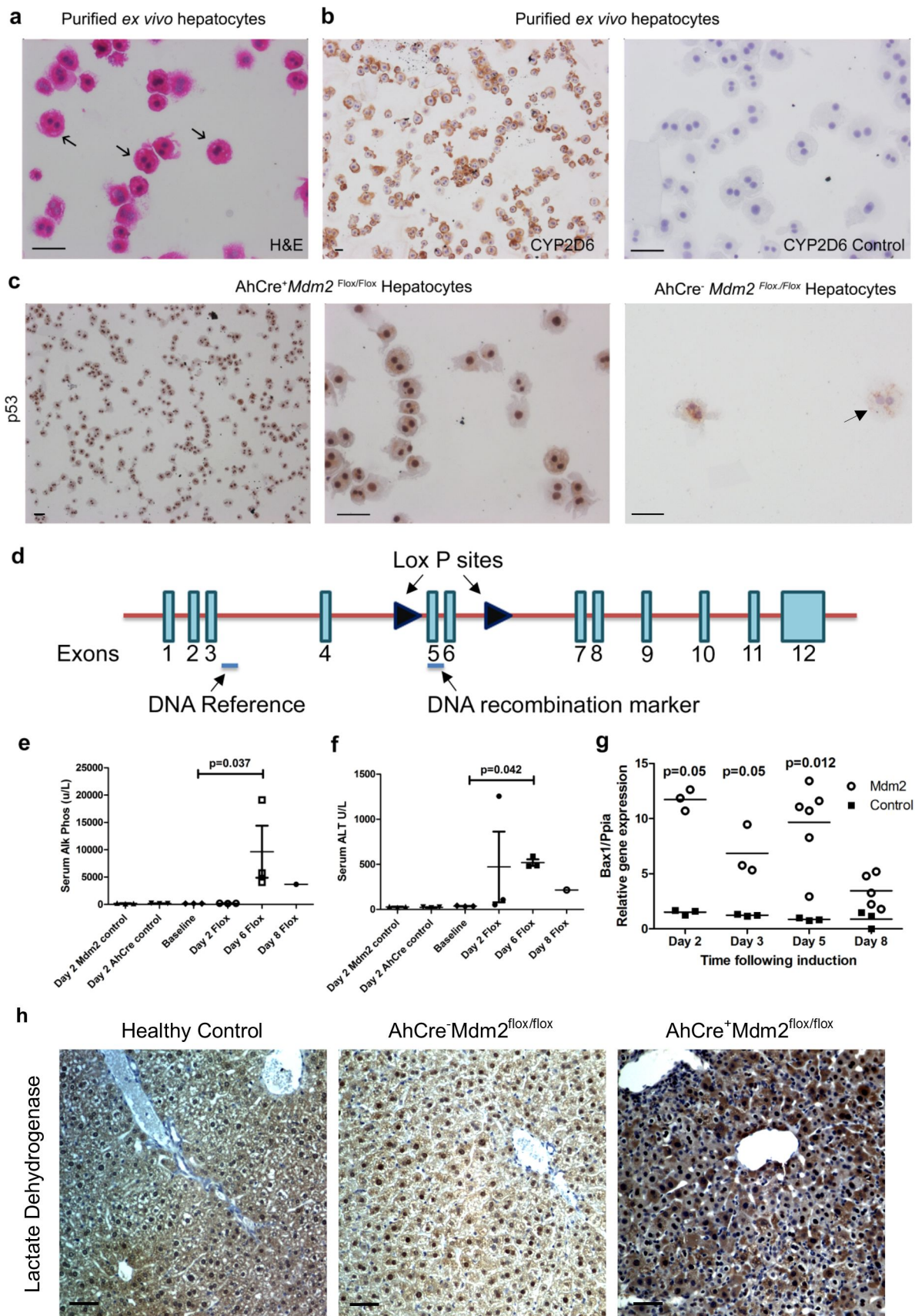
Supplementary table 2: List of antibodies used

Antibodies used for antigen detection in the current study are provided together with mode of tissue fixation, method of antigen retrieval and working dilution. Formalin = fixation for 6 hours in 10% formalin in PBS, NaC = 100mM Sodium Citrate pH 6.0, and Tris EDTA = 100mM Tris EDTA pH 9.0.

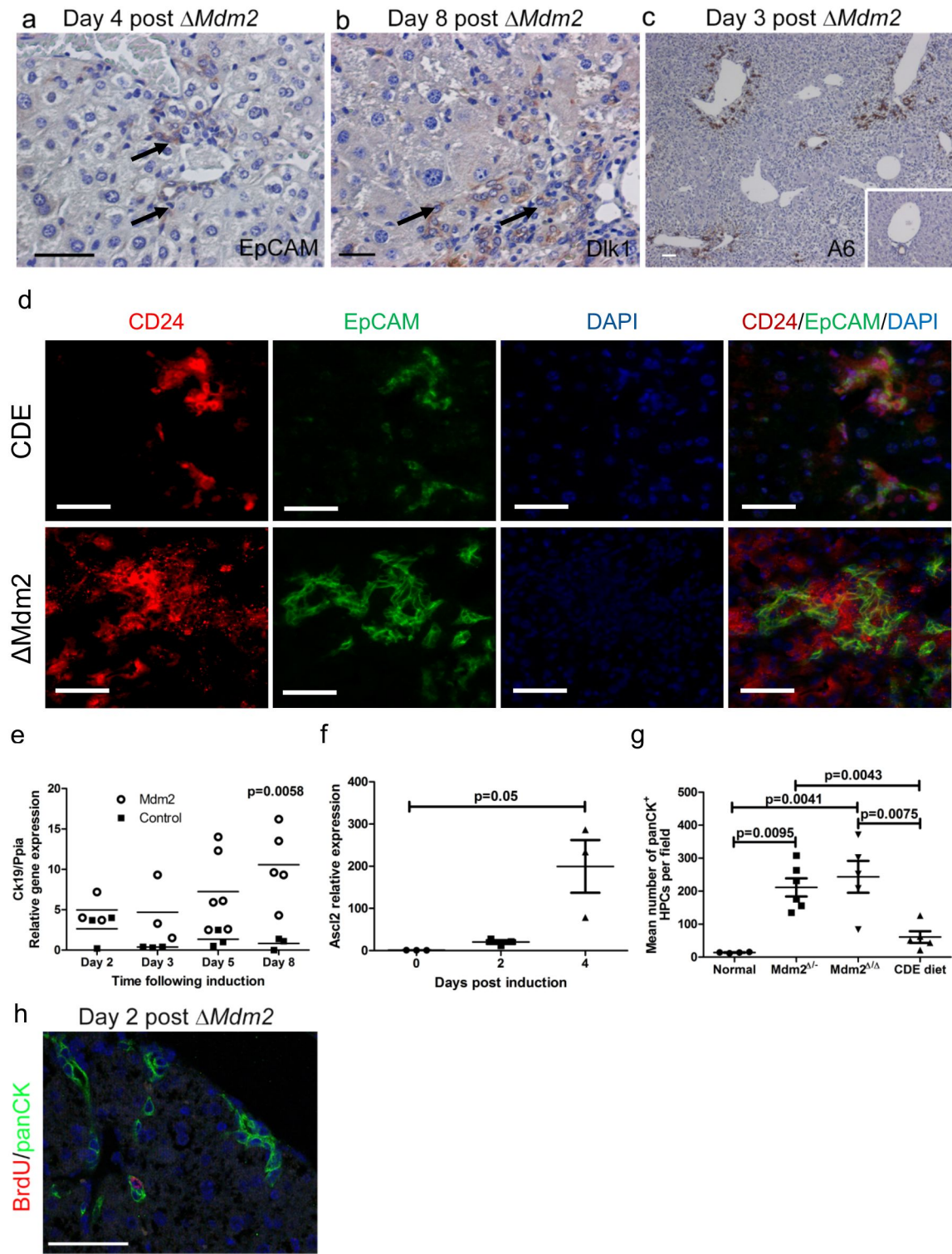
Supplementary 1



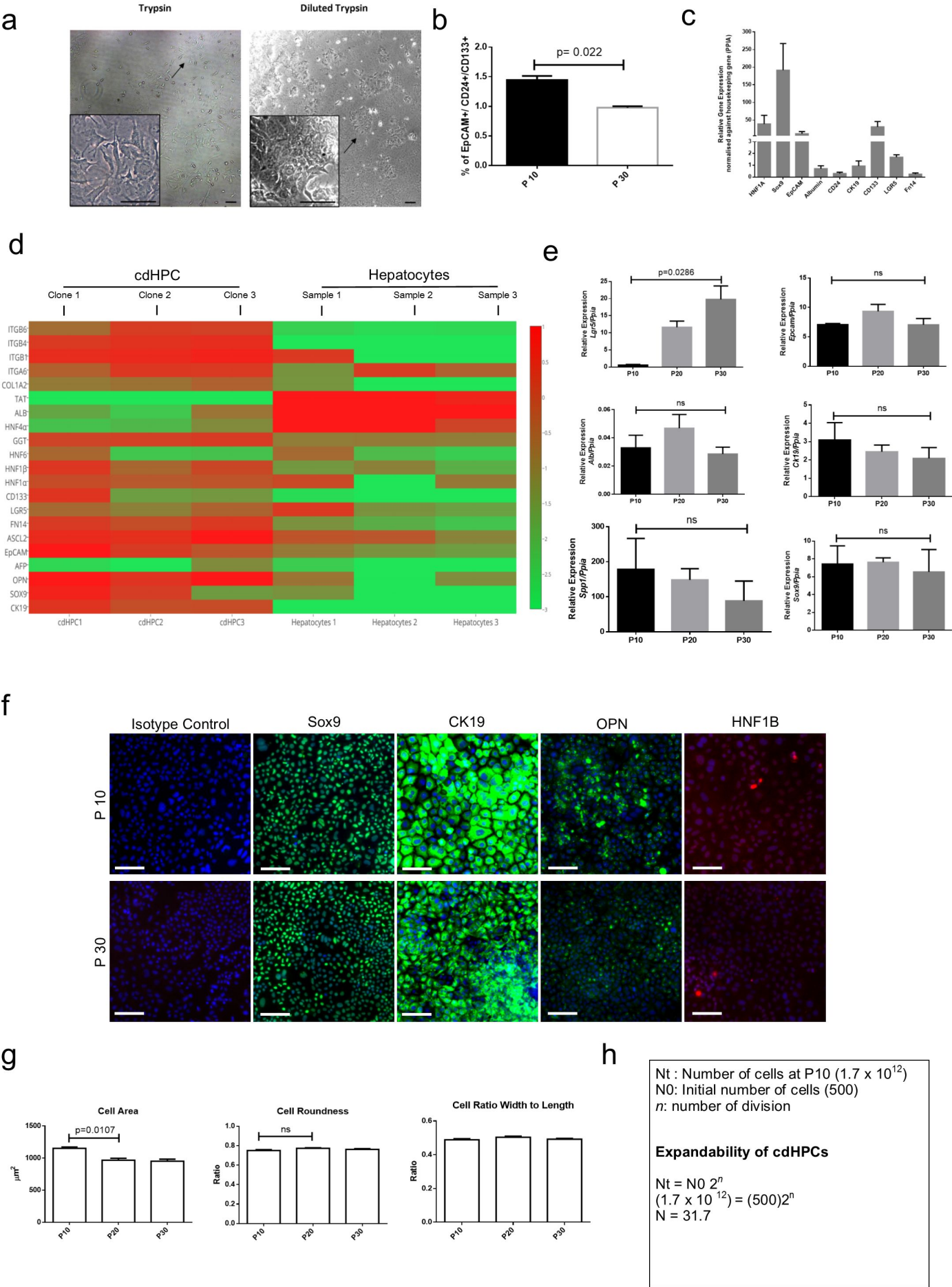
Supplementary 2



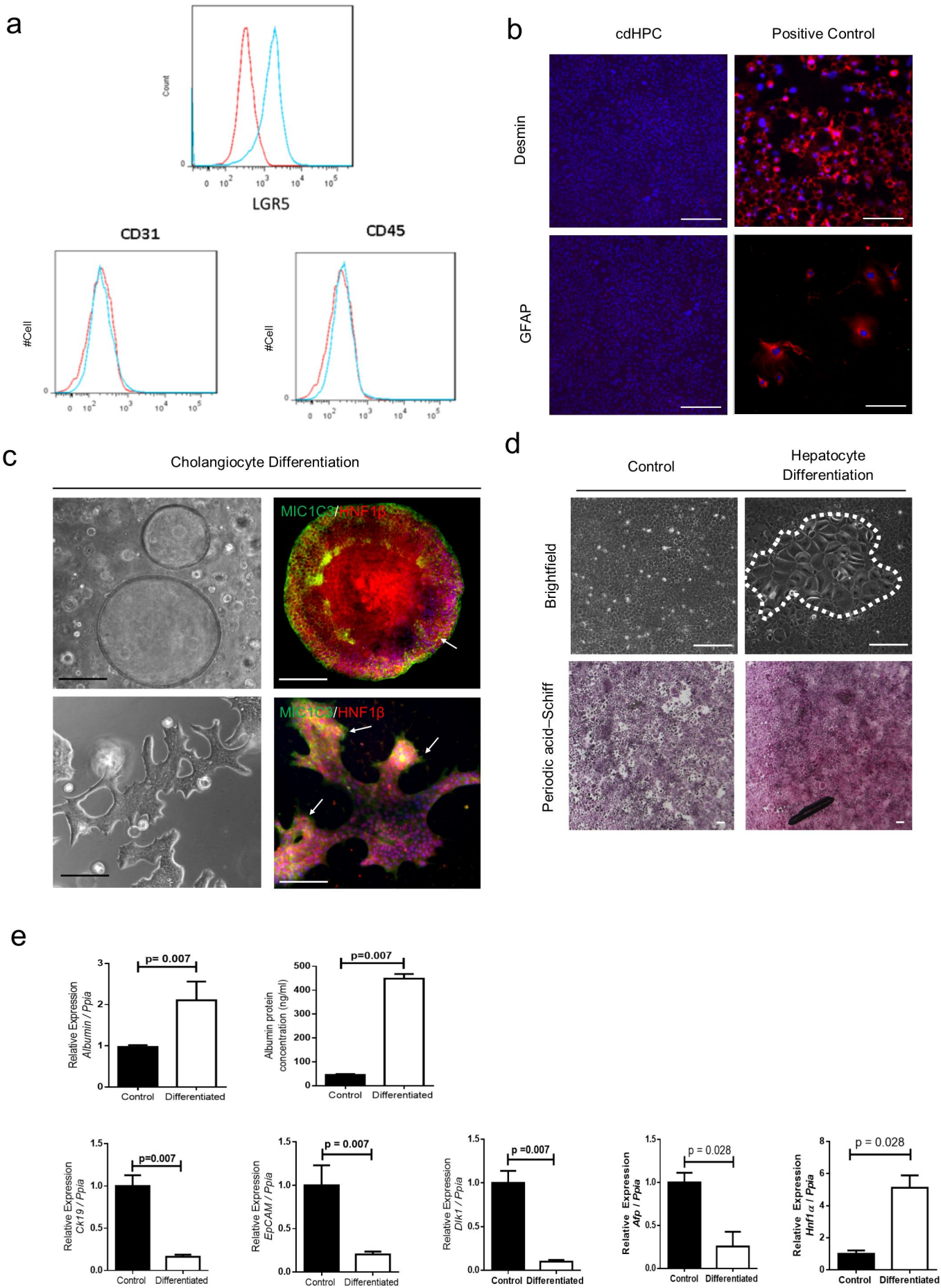
Supplementary 3



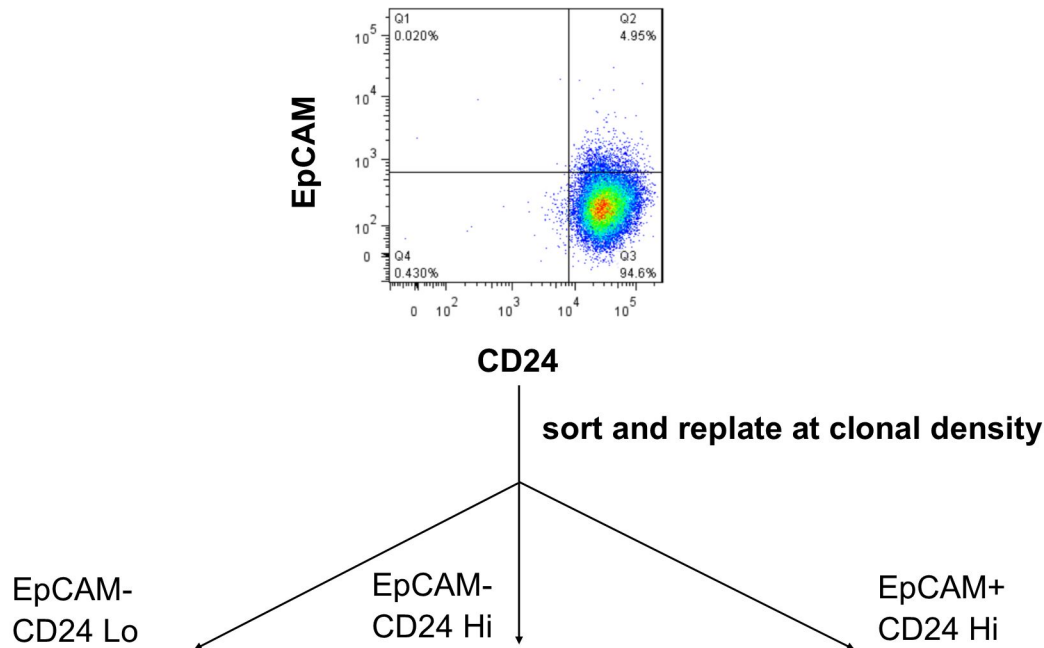
Supplementary 4



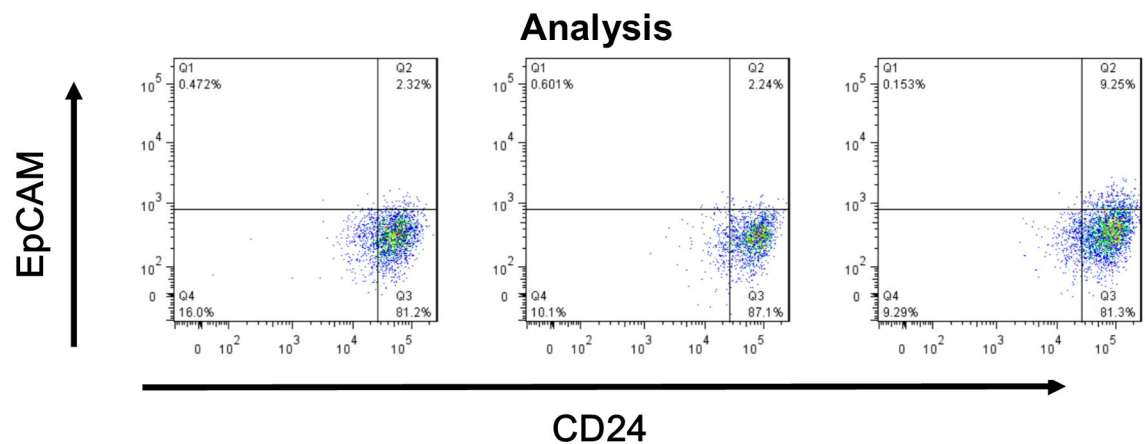
Supplementary 5



a

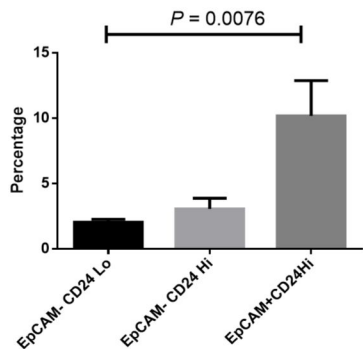


b

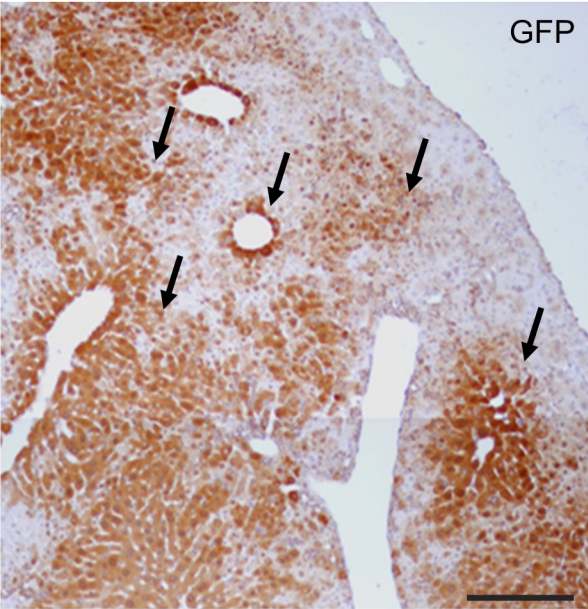


c

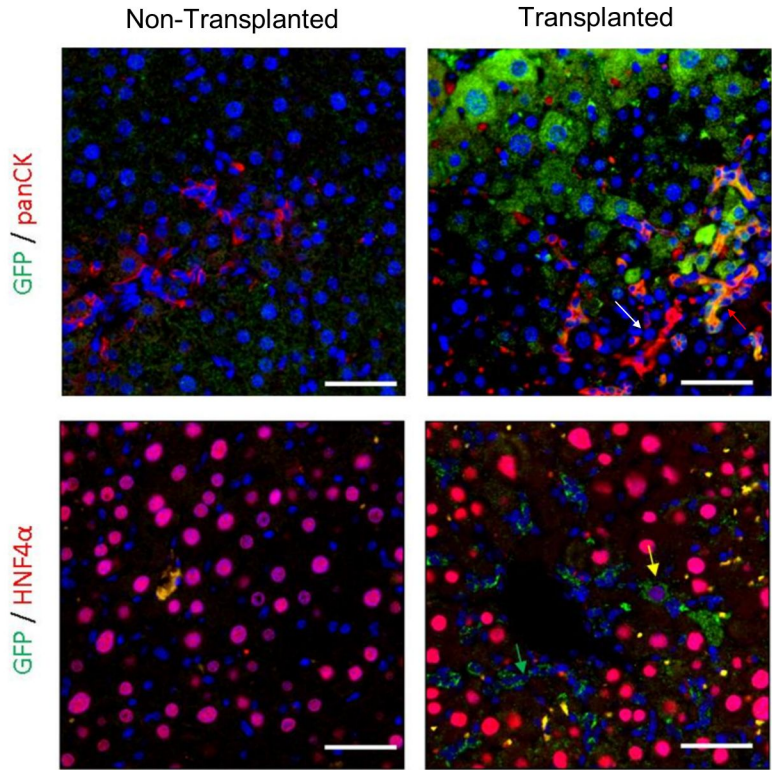
EpCAM+ CD24+ Population of Secondary clones



a



b



c

